TECHNICAL UNIVERSITY OF CLUJ-NAPOCA

ACTA TECHNICA NAPOCENSIS

Series: Applied Mathematics, Mechanics, and Engineering
Vol. 69, Issue II, June, 2026

SUSTAINABLE MANAGEMENT OF INDOOR AIR QUALITY: A NUMERICAL STUDY OF HEAT AND MASS TRANSFER IN VENTILATED CAVITIES USING THE LB-MRT METHOD

Ahmed ADJAL, Venera-Stanca NICOLICI, Ioana IONEL, Daniel BISORCA

Abstract: *This research explores the transport of heat and chemical species within a ventilated rectangular enclosure using numerical modeling. The analysis is performed by applying the Lattice Boltzmann Method with Multiple Relaxation Time (LBM-MRT) approach. The primary objective is to optimize indoor air conditions and the effectiveness of contaminant extraction. A distinctive aspect of this study is incorporating sustainability management frameworks into the numerical evaluation. The physical model includes a central reactive porous barrier with adjustable permeability to simulate filtration processes. By investigating various ventilation approaches for residential settings, the study evaluates thermal comfort and air purification. The analysis utilizes flow patterns, thermal distributions, and concentration gradients, alongside performance metrics such as depollution rate and air quality indicators.*

Keywords: *Lattice Boltzmann Method (LBM-MRT), reactive porous medium, mixed convection, indoor air quality (IAQ), depollution efficiency, displacement ventilation.*

1. INTRODUCTION

Poor air quality management is a major risk factor for human health, whether it occurs during outdoor or indoor exposure. Mitigating the significant risk posed by poor indoor air quality requires a proactive management approach, transforming the built environment from a passive container into an actively managed asset for human well-being.

Indoor air quality (IAQ) is of primary importance because people spend approximately 80% of their time indoors. Poor IAQ reduces occupant comfort, productivity and cognitive performance [1]. Because of its significant impact on building occupants' productivity, well-being, and health, the idea of indoor air quality has taken center stage in discussions of the built environment [2]. Therefore, one can consider that indoor air quality analysis is a condition for achieving sustainable management. For example, in universities, numerous health issues, such as respiratory issues, allergies, and diminished cognitive function, have been connected to poor indoor air quality, and these issues can have a detrimental effect on faculty performance and student learning outcomes [3-5]. The work environment, resources available, and physical and mental health are some of the elements that affect human productivity [6]. A multifaceted skill in many fields, creativity is impacted by the social and physical surroundings [7].

Human activity, insufficient ventilation, a lack of air conditioning systems, and innumerable materials, chemicals, and gases are the main causes of indoor pollution [8]. Therefore, maintaining a high level of indoor environmental quality in homes is becoming more and more crucial to safeguarding health.

Sustainable management of indoor air quality focuses on reducing pollutants at the source, improving ventilation efficiency, and using eco-friendly materials to create healthier indoor environments. By integrating energy-efficient systems with proper air filtration and maintenance, it ensures long-term indoor air quality without compromising environmental sustainability.

Sustainable management of indoor air quality emphasizes source control, energy-efficient ventilation, and the use of environmentally friendly materials to promote healthier indoor environments. This approach ensures long-term air

Received: 13.04.26; **Similarities**: 16.04.26: **Reviewed**: 13.04. /13.04.26: **Accepted 1**0.06.26.

quality while aligning with broader goals of environmental sustainability.

Although previous studies investigated natural and forced convection in ventilated enclosures and porous medium effects [9–15], there is limited work combining reactive porous layers with a parametric Lattice Boltzmann Method with Multiple Relaxation Time (LBM-MRT) analysis that simultaneously quantifies heat transfer, pollutant removal (depollution efficiency) and an IAQ index for displacement ventilation configurations. This study fills that gap by introducing a centrally located reactive porous partition and performing a systematic parametric study of *Re, Ra, Da, Ri* and the dimensionless chemical reaction rate A_K.

The objectives of this work are to quantify how porous-layer permeability (*Da*), and chemical reaction rate (A_K) affect pollutant removal, to evaluate thermal performance (*Nu*) under mixed convection, to propose a practical IAQ index and to recommend optimal ventilation parameters for improved IAQ and energy efficiency. Key findings are the reactive porous layer improves depollution substantially for low *Da*; chemical reaction reduces pollutant residence time but minimally affects temperature fields; and combined operation can lead to energy savings under specific *Re–Ra* regimes.

The phenomena of simultaneous heat and mass transfer in ventilated cavities continue to attract significant academic interest, owing to their widespread integration in numerous practical applications [9-11]. The novel aspect of this research involves the strategic placement of a chemically active porous partition within the enclosure to regulate flow and transport processes [12-14]. This component functions as a filtration medium designed to entrap contaminants. The primary objective of this research is to evaluate how the integration of a chemically active porous divider affects both the airflow dynamics and the overall purification efficiency within the indoor space.

The Darcy-Brinkman framework was utilized to characterize the fluid flow within the porous architecture, revealing that enclosure tilt, thermal Rayleigh number (*Ra*), and permeability (Darcy number) significantly influence convective heat and moisturized transport. Similarly, Oztop et al. achieve the same conclusion [12]. By adopting the Brinkman-Forchheimer model, this research examines the interaction between thermal gradients and fluid flow in a cavity that is partially open and subjected to discrete heating zones.

The mesoscopic nature of the Lattice Boltzmann Method (LBM) makes it particularly adept at handling complicated transport phenomena. This technique is highly regarded for its numerical resilience and the ease with which it incorporates complex boundaries in porous media. For convective heat transfer, Liu et al. [15] incorporated porous medium effects into a Lattice Boltzmann-Multiple Relaxation Time (LB-MRT) model via a forcing factor and modified equilibrium moments. For the numerical solution, the velocity distribution is modeled using the D2Q9 lattice scheme, while the temperature distribution is resolved through the D2Q5 lattice arrangement.

Emerging as an evolution of lattice gas cellular automata, the Lattice Boltzmann Method provides a robust framework characterized by high physical fidelity and streamlined computational performance, especially for intricate boundary constraints. This approach has gained substantial traction in fluid dynamics, evolving into a primary numerical tool for complex simulations. In the present work, the governing equations are resolved using the Multiple Relaxation Time scheme to ensure numerical stability. The findings highlight a profound sensitivity of the flow field to fluctuations in temperature magnitude, employing periodic boundary treatments analogous to those developed in the studies by Arab et [16-17]. To analyze indoor thermal stability, this study utilizes the Rayleigh-Bénard convection framework to model heat transfer in an enclosure heated from below, specifically focusing on its implications for occupant comfort.

The scopes of the research are (i) to investigate the coupled thermal and mass transport phenomenon, and (ii) to provide a rigorous basis for the numerical simulations. One considers further introducing shortly the governing partial differential equations and their respective dimensionless forms. The set of boundary conditions applied to the ventilated cavity is also rigorously defined.

2. NUMERICAL MODELING AND PROBLEM FORMULATION

A numerical study is performed on the mixed double-diffusion phenomena within a ventilated cavity of aspect ratio 2. The ventilation process is facilitated by air exchange through diagonal ports of H/10 diameter. Regarding the boundary conditions, the right boundary serves as a constant heat source (Th), while all other enclosure surfaces are defined as insulated and impermeable to mass flux (see Fig. 1).

Some assumptions are considered to simplify the mathematical equations governing this model, assuming that: (i) the fluid (air) is Newtonian, (ii) all thermophysical properties of the fluid are assumed to be temperature-independent, excepting the density variation in the buoyancy term, which uses the Boussinesq approximation, assuming a linear temperature dependence [18]:

$$(\rho - \rho_\infty) = -\beta.\rho_\infty(T - T_\infty) \quad (1)$$

where β represents the volumetric expansion coefficient.

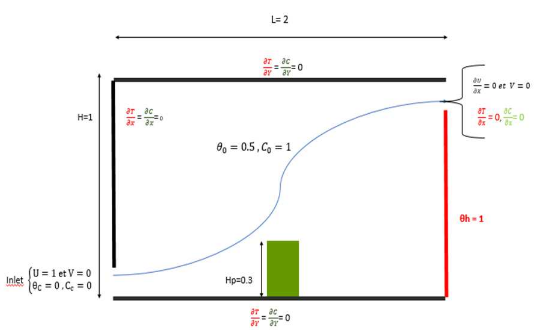

Fig. 1. Schematic representation of the physical domain and the implemented non-dimensional boundary conditions.

In this analysis, the fluid motion is treated as laminar and incompressible within a uniform, isotropic porous medium. The model assumes local thermal equilibrium and investigates the dual diffusion of energy and pollutants. Additionally, a linearized version of the Arrhenius law is employed to simulate the chemical reaction mechanisms [13], valid for small maximum temperature gradients.

3. SYSTEM OF GOVERNING EQUATIONS AND SCALING

Based on the generalized Darcy-Brinkman-Forchheimer model, the dimensional conservative equations of momentum, heat, and mass for the porous zone were applied. The continuity equation expresses the conservation of mass for a moving fluid [19]. It asserts that for any elementary volume, the net mass flow rate through its surface equals the time rate of change of mass inside the volume. It is defined as follows:

$$\frac{d\rho^*}{dt^*} + \nabla^* u^* = 0 \quad (2)$$

The momentum equation [20] is:

$$\frac{\partial u^*}{\partial t^*} + (u^* \cdot \nabla^*)\left(\frac{u^*}{\varepsilon}\right) = -\frac{1}{\rho}(\varepsilon p^*) + \nu_{eff}\nabla^{*2}u^* + F^* \quad (3)$$

The energy equation [21] is:

$$\frac{\partial T^*}{\partial t^*} + \nabla^* \cdot (T^* u^*) = \alpha_{eff}\nabla^{*2}T^* \quad (4)$$

The diffusion equation [21] is:

$$\frac{\partial C^*}{\partial t^*} + \nabla^* \cdot (C^* u^*) = D_{eff}\nabla^{*2}C^* + a_k\left(c^*_{eq}(T^*) - C^*(T^*)\right) \quad (5),$$

For the term $a_k(c^*_{eq}(T^*) - c^*(T^*))$ relation [13] is applied, where ε, ν_{eff} , α_{eff} and a_k denote the material's porosity alongside its transport and kinetic coefficients (thermal and reaction). The variable F^* signifies the aggregate resistive and driving effects originating from the porous matrix and auxiliary fields, which is formulated as follows:

$$F^* = -\frac{\varepsilon\nu}{K}u^* - \frac{1.75}{\sqrt{150\varepsilon K}}|u^*|u^* + \varepsilon G^* \quad (6)$$

$$G^* = g(\beta_T(T^* - T^*_c) + \beta_C(C^* - C^*_c) \quad (7)$$

4. DIMENSIONLESS EQUATIONS

The equations, describing the experiment, are dimensionless and follow the reduced variables: $X = \frac{x^*}{H}, Y = \frac{y^*}{H}, U = \frac{u^*}{U_0}, V = \frac{v^*}{U_0}, P = \frac{p^*}{\rho U_0^2}, \theta = \frac{T^* - T_c}{\Delta T_{ref}}, C = \frac{C^* - C_c}{\Delta_{ref}}, \Delta T_{ref} = T_h - T_c, \Delta C_{ref} = C_o - C_c, t = \frac{t*}{H/U_0}$ (8)

The dimensionless form of these equations allows the appearance of the following dimensionless control parameters:

Prandtl number

$$Pr = \frac{\upsilon}{\alpha} \quad (9)$$

Reynolds number

$$Re = \frac{U_0 H}{\upsilon} \quad (10)$$

Rayleigh number

$$Ra = \frac{g\beta\Delta T_{ref} H^3}{\upsilon\alpha} \quad (11)$$

Darcy's number

$$Da = \frac{K}{H^2} \quad (12)$$

Reaction rate

$$A_k = \ a_k \frac{H}{U_0} \quad (13)$$

Lewis number

$$Le = \frac{D_{eff}}{\alpha} \quad (14)$$

Richardson number

$$Ri = \frac{Ra}{P_r \times Re^2} \quad (15)$$

The mathematical representation of the flow in its dimensionless form, considering the fluid-only zone and the Cartesian reference frame, is given by the continuity equation:

$$\frac{\partial U}{\partial X} + \frac{\partial V}{\partial Y} = 0 \quad (16)$$

The equation of quantity of motion along X and Y is:

$$\frac{\partial U}{\partial t} + \left[U\frac{\partial U}{\partial X} + V\frac{\partial U}{\partial Y}\right] = -\frac{\partial P}{\partial X} + \frac{1}{\text{Re}}\left(\frac{\partial^2 U}{\partial X^2} + \frac{\partial^2 U}{\partial Y^2}\right) \quad (17)$$

$$\frac{\partial V}{\partial t} + \left[U\frac{\partial V}{\partial X} + V\frac{\partial V}{\partial Y}\right] = -\frac{\partial P}{\partial Y} + \frac{1}{\text{Re}}\left(\frac{\partial^2 V}{\partial X^2} + \frac{\partial^2 V}{\partial Y^2}\right) + \text{Ri}(\theta + NC) \quad (18)$$

The energy equation is:

$$\frac{\partial \theta}{\partial t} + U\frac{\partial \theta}{\partial X} + V\frac{\partial \theta}{\partial Y} = \frac{1}{\text{RePr}}\left(\frac{\partial^2 \theta}{\partial X^2} + \frac{\partial^2 \theta}{\partial Y^2}\right) \quad (19)$$

The diffusion equation is:

$$\frac{\partial C}{\partial t} + U\frac{\partial C}{\partial X} + V\frac{\partial C}{\partial Y} = \frac{1}{LeRePr}\left(\frac{\partial^2 C}{\partial X^2} + \frac{\partial^2 C}{\partial Y^2}\right) \quad (20)$$

In the porous zone, the equations are as follows.

The continuity equation is:

$$\frac{\partial U}{\partial X} + \frac{\partial V}{\partial Y} = 0 \quad (21)$$

The equation of momentum is:

$$\frac{\partial U}{\partial t} + \left[U\frac{\partial}{\partial X}\left(\frac{U}{\varepsilon}\right) + V\frac{\partial}{\partial Y}\left(\frac{U}{\varepsilon}\right)\right] = -\frac{\partial \varepsilon P}{\partial X} - \frac{1}{\text{DaRe}}U + \frac{1}{\text{Re}}\left(\frac{\partial^2 U}{\partial X^2} + \frac{\partial^2 U}{\partial Y^2}\right) - \frac{1.75}{\sqrt{150}}\frac{(U^2+V^2)^{\frac{1}{2}}}{\sqrt{Da}}U \quad (22)$$

$$\frac{\partial V}{\partial t} + \left[U\frac{\partial}{\partial X}\left(\frac{V}{\varepsilon}\right) + V\frac{\partial}{\partial Y}\left(\frac{V}{\varepsilon}\right)\right] = -\frac{\partial \varepsilon P}{\partial Y} - \frac{1}{\text{DaRe}}V + \frac{1}{\text{Re}}\left(\frac{\partial^2 V}{\partial X^2} + \frac{\partial^2 V}{\partial Y^2}\right) + \text{Ri}(\theta + NC) - \frac{1.75}{\sqrt{150}}\frac{(U^2+V^2)^{\frac{1}{2}}}{\sqrt{Da}}V \quad (23)$$

The energy equation is:

$$\frac{\partial \theta}{\partial t} + \frac{\partial (U\theta)}{\partial X} + \frac{\partial (V\theta)}{\partial Y} = \frac{1}{RePr}\left(\frac{\partial^2 \theta}{\partial X^2} + \frac{\partial^2 \theta}{\partial Y^2}\right) \quad (24)$$

The diffusion equation is:

$$\varepsilon\frac{\partial C}{\partial t} + U\frac{\partial C}{\partial X} + V\frac{\partial C}{\partial Y} = \frac{1}{LeRePr}\left(\frac{\partial^2 C}{\partial X^2} + \frac{\partial^2 C}{\partial Y^2}\right) + A_k(\theta - C) \quad (25)$$

5. THE LATTICE BOLTZMANN METHOD

Numerical solutions in this work are obtained using the Lattice Boltzmann Method (LBM) with a Multiple Relaxation Time (MRT) scheme. The preference for this technique stems from its robust numerical performance and its inherent ability to accurately simulate heat and fluid flow in complex geometric domains.

To capture the dynamics of double-diffusion in a cavity featuring a porous reactive zone, we employ the LBM-MRT strategy. This mesoscopic technique stands out from conventional Navier-Stokes solvers due to its superior performance in parallel environments and its inherent stability. Such advantages are crucial for accurately modeling the exchange processes at the fluid-porous boundary in this specific configuration.

Unlike standard computational fluid dynamics (CFD) techniques, the LBM provides a mesoscopic perspective that bridges the gap between microscopic particle movement and macroscopic flow behavior, offering a unique alternative for complex fluid simulations. Its development stems from the convergence of statistical physics and cellular automata theory [22, 23]. The method is based on the Boltzmann equation, formulated in 1872, which describes the spatio-temporal evolution of a particle distribution function, *f*. This function, *f*(*x*,*v*,*t*) represents the probability density associated with particles traveling at a defined velocity at any specific location within the domain at time, according following relation:

$$\frac{\partial f}{\partial t} + c\frac{\partial f}{\partial t} + \frac{F}{m}\frac{\partial f}{\partial c} = \Omega(f)cool \quad (26)$$

The Boltzmann equation's collision operator accounts for particle interactions. Its value determines the system's behavior: if zero, motion is driven only by the external force *F*; if non-zero, the collision model governs the evolution.

The Chapman-Enskog expansion [24], later validated experimentally, is a rigorous theoretical foundation connecting the Boltzmann kinetic theory to the Navier-Stokes equations, which was initially developed. Nevertheless, the mathematical intricacy of the original collision term posed significant challenges for numerical implementation. A breakthrough occurred in 1954, when Bhatnagar, Gross, and Krook proposed the BGK approximation, which substantially streamlined the collision process [25]. Within this framework, molecular interactions are modeled as a restorative process toward a state of local equilibrium. This conceptual shift transformed the Boltzmann equation into a feasible tool for fluid dynamics modeling. Although the BGK operator established the essential mathematical basis for what would become the Lattice Boltzmann Method, its transition into a functional numerical algorithm was realized only after subsequent advancements in discrete computational schemes.

5.1 Maxwell-Boltzmann equilibrium distribution function

The function is:

$$\left(\frac{\partial f}{\partial t}\right)_{coll} = 0 \tag{27}$$

Such a function therefore verifies:

$$f_i^{eq} = \omega_i \rho \left[1 + \frac{\vec{e}_i \cdot \vec{u}}{c_s^2} + \frac{(\vec{e}_i \cdot \vec{u})^2}{2\varepsilon c_s^4} - \frac{\vec{u} \cdot \vec{u}}{2\varepsilon c_s^2}\right] \tag{28}$$

where ω_i = network constants, Cs = speed of sound, $\vec{u}$ = speed vector.

5.2 Numerical Discretization of the LBM Framework

The Lattice Boltzmann Method serves as a robust tool for investigating the coupled phenomena of fluid dynamics, thermal energy, and mass transport. In this approach, the fluid is modeled as a discrete collection of particles that traverse the grid along predefined lattice directions with specific velocities. The fundamental interaction involves particle collisions at the lattice sites followed by a migration step. The evolution of the particle distribution functions, which represent the probability density of finding a particle with a given velocity at a specific node, is governed by the discrete Boltzmann equation. To account for external influences, an appropriate source term is integrated into the governing equations:

$$f_j(x_i + v_i \Delta \mathrm{t}, \mathrm{t} + \Delta \mathrm{t}) = f_j(x_i, t) + \Omega_j(f)(x_i, t) \tag{28a}$$

In the BGK approximation, Bhatnagar, Gross, and Krook developed a simplified model of the collision operator in 1954 [25].

$$\Omega = \omega[\mathrm{f}^{eq} - \mathrm{f}] = \frac{1}{\tau}[\mathrm{f}^{eq} - \mathrm{f}] \tag{29}$$

$$\omega = \frac{1}{\tau} \tag{30}$$

where: ω is the collision frequency and τ is Relaxation factor.

In this framework, the local equilibrium function is modeled based on Maxwell–Boltzmann statistics. Thus, the BGK-based Boltzmann equation, assuming no external body forces, takes the following discrete form:

$$\frac{\partial f}{\partial t} + c.\nabla f = \frac{1}{\tau}[\mathrm{f}^{eq} - \mathrm{f}] \tag{31}$$

To represent the particle transport in a discretized velocity space, the following velocity vectors are defined (the term on the left refers to advection, that on the right refers to collision):

$$\frac{\partial f_i}{\partial t} + c_i.\nabla f_i = \frac{1}{\tau}\left[\mathrm{f}_i^{eq} - \mathrm{f}_i\right] \tag{32}$$

5.3 Modeling with Multiple Relaxation Time Scales

To circumvent LBGK limitations like numerical instability and a fixed Prandtl number, d'Humières introduced the Multiple-Relaxation-Time (MRT) model. It improves stability and flexibility, by performing the collision in an orthogonal moment space, using independent relaxation times for different physical moments. The corresponding collision term is [26]:

$$\Omega = -M^{-1}S[m(x,t) - m^{eq}(x,t)] \tag{33}$$

Therefore, the Boltzmann equation is:

$$f_i(x + c_i \Delta t, t + \Delta t) - f_i(x,t) = -M^{-1}S[m(x,t) - m^{eq}(x,t)] \tag{34}$$

where Ω is the collision matrix.

The collision phase is executed within the moment domain, allowing for a more flexible relaxation process. A linear transformation, defined by a square matrix M, maps the discrete distribution functions *fi* to the moment vector $m(m_0, m_1, \ldots, m_8)^T$:

$$m = (m_0, m_1, \ldots, m_8)^T = \left(\rho, E, \varepsilon, j_x, q_x, j_y, q_y, p_{xx}, p_{xy}\right)^T \quad (35)$$

The correspondence between the velocity and momentum spaces is performed by linear transformation as follows:

$$m = Mf \quad (36)$$

$$f = M^{-1}m \quad (37)$$

6. SIMULATION RESULTS AND DATA INTERPRETATION

This part of the study is dedicated to showcasing the simulation findings obtained through the MRT-based lattice Boltzmann approach and analyzing the observed phenomena. Each subsection focuses on a key physical aspect: flow structure, thermal field, and mass field, to highlight how the reactive porous layer and other control parameters influence ventilation performance and depollution efficiency. The novelty lies in quantitatively correlating parameters (*Da, A_k, Re, Ra, Ri*) with system performance, a combined analysis rarely conducted for reactive porous media using LBM-MRT.

6.1 Flow structure

The flow structure is primarily controlled by the Darcy number (*Da*). A high *Da* (10^{-2}) makes the porous layer transparent, while a low *Da* (10^{-6}) makes it act as an impermeable wall. At higher *Re* and *Ri*, high permeability induces recirculation, redirecting the jet. Low permeability with high *Re* generates vortices and causes short-circuiting flow to the outlet. Notably, the chemical reaction rate (A_k) has no significant impact on the flow (see Figures 2 and 3).

6.2 Thermal field

The chemical reaction rate has negligible influence on the thermal distribution. In all simulations, isotherms concentrate mainly in the right compartment of the cavity.

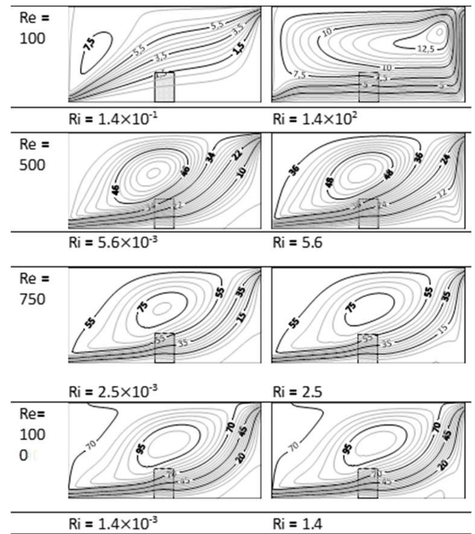

Fig. 2. Streamlines *Da*=10^ (-2), A_K=0, *Hp*=0.3.

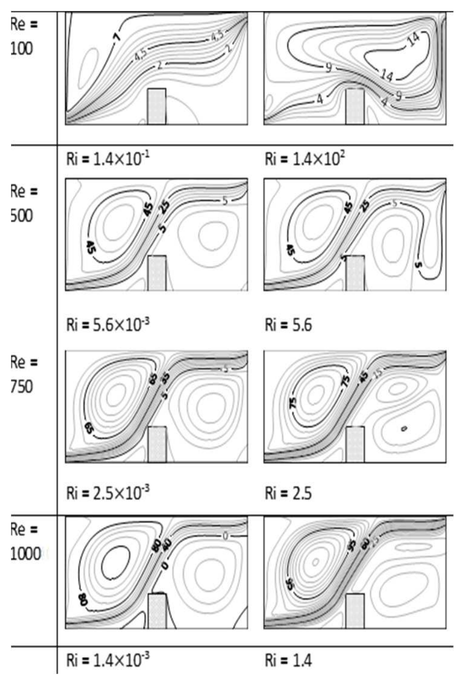

Fig. 3. Streamlines *Da*=10^ (-6), A_K=1, *Hp*=0.3.

For low *Re* and R_i: (i) With high permeability (*Da* = 10^{-2}), isotherms are open near the hot wall. (ii) At a diminished permeability level (*Da* = 10^{-6}), the porous medium exhibits solid-like behavior, significantly impeding fluid penetration. Consequently, the isotherms are densely packed in the vicinity of this layer, indicating steep thermal gradients, as shown in Figures 4 and 5.

In regimes characterized by elevated Reynolds (*Re*) and Richardson (*Ri*) numbers, where natural convection prevails, a significant compression of isotherms occurs. This leads to a thinning and flattening of the thermal boundary layer adjacent to the heated surface, which in turn intensifies the local temperature gradients. Conversely, at a minimal Darcy number ($Da = 10^{-6}$), the porous medium exerts a profound resistive effect; by obstructing the infiltration of cooler air into certain zones, it maintains a more dispersed or 'open' configuration of the isotherms.

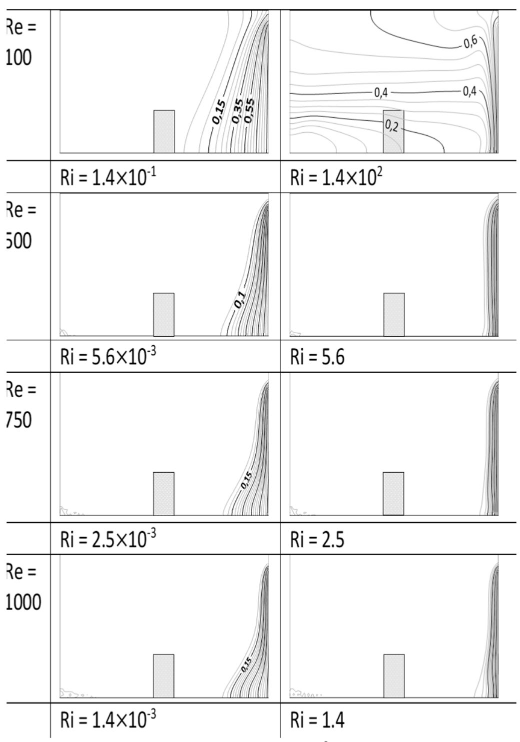

Fig. 4. Isotherms Da=10^{-2}, A_K=0, Hp=0.3.

In summary, the flow visualization confirms that the porous layer permeability (*Da*) strongly governs the global circulation pattern, controlling the formation and location of recirculation zones. Overall, thermal analysis confirms that buoyancy (*Ra*) dominates heat transfer. The chemical reaction has a negligible thermal effect, while the porous layer's permeability locally alters temperature gradients.

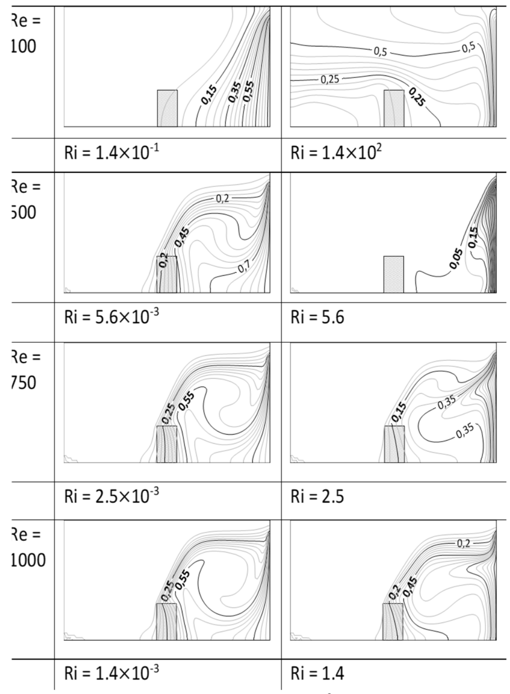

Fig. 5. Isotherms Da=10^{-6}, A_K=1, Hp=0.3.

6.3 Mass field

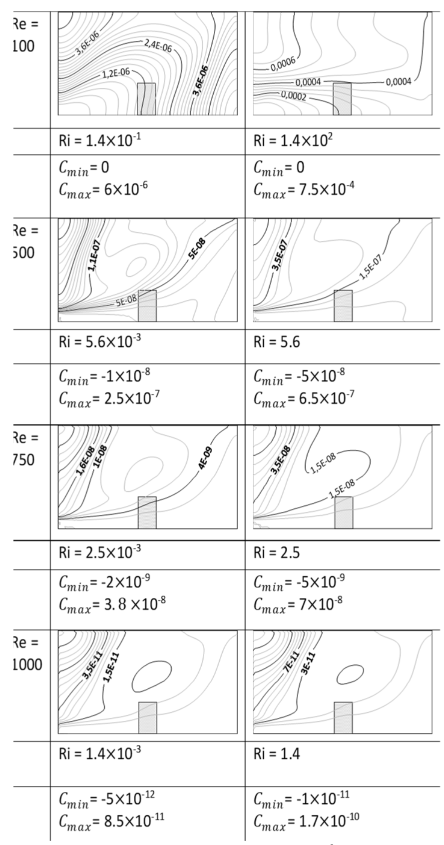

Fig. 6. Iso-concentration Da=10^{-6}, A_K=1, Hp=0.3.

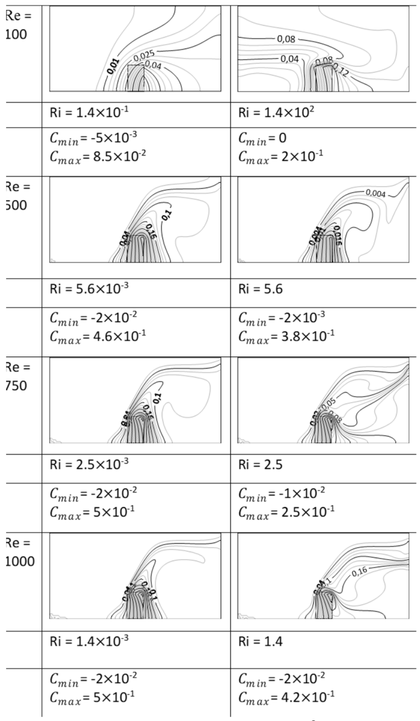

Fig. 7. Iso-concentration Da=10^{-2}, A_K=0, Hp=0.3.

For high permeability ($Da = 10^{-2}$) and $A_k = 0$, iso-concentrations are open and widespread. Increasing *Re* creates a cleaner zone in the first compartment, consistent with the flow field.

Introducing a reactive porous layer significantly enhances depollution, especially at low Darcy numbers ($Da = 10^{-6}$) and high A_k. In these regimes, iso-concentrations tighten, indicating strong concentration gradients. Without reaction (A_k=0), pollutant reduction is minimal and driven solely by forced convection. In contrast, a reactive layer chemically reduces pollutant levels, confirming its depollution efficiency.

7. INDOOR AIR QUALITY INDEX (IAQ)

Sustainable IAQ management integrates pollutant control, efficient ventilation, and eco-friendly materials to maintain healthy indoor environments. It balances occupant well-being with long-term environmental sustainability. IAQ values are evaluated at steady state:

- For high permeability ($Da = 10^{-2}$):

At low Reynolds (Re < 500), chemical reaction improves IAQ in both zones. At higher *Re*, the influence of the chemical reaction becomes negligible, leading to a convergence of the IAQ profiles, where the curves exhibit an identical trend. With strong heating ($Ra = 10^6$), the chemical effect persists up to $Re \approx 750$.

- For low permeability ($Da = 10^{-6}$):

Evidence of the chemical reaction is consistent for all Re values, with its most significant contribution observed in the initial chamber. In this region, the dual action of reaction-driven decay and air exchange enhances the overall depollution efficiency, leading to a more rapid decline in contaminant concentration (Figure 8).

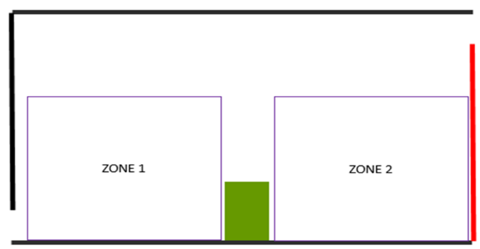

Fig. 8. Diagram showing the occupancy zones before and after the porous partition.

This analysis highlights that sustainable IAQ management can be achieved by optimizing both permeability and chemical reactivity, enabling cleaner air distribution and potential energy savings through reduced ventilation demand, as shown in Figures 9 and 10.

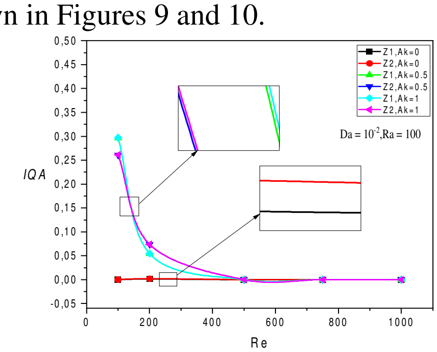

Fig. 9. The Indoor Air Quality Index (IAQ), Da=10^{-2}, Ra=100.

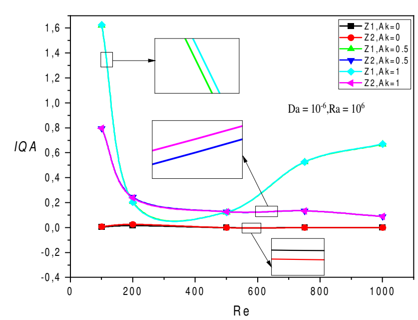

Fig. 10. The Indoor Air Quality Index (IAQ), Da=10^{-6}, Ra=10^{6}.

8. CONCLUSION

The results of this computational investigation provide critical insights into how porous medium parameters influence ventilation performance. The following summary encapsulates the major contributions of this study, specifically focusing on the synergy between fluid transport and environmental sustainability in indoor spaces.

The present study investigated the synergistic effects of ventilation and chemical reaction on air quality within a rectangular domain featuring a porous partition. Utilizing a displacement ventilation flow setup, the analysis focused on how geometric and physical constraints, specifically the Darcy and Reynolds numbers, modulate thermal efficiency and pollutant removal. The findings provide a detailed mapping of flow regimes and transport phenomena under mixed convection conditions, across varying levels of buoyancy-driven convection and reaction-driven decay.

The main findings can be summarized as:

- **Effect of Darcy number (*Da*):** Variations in the permeability of the porous layer exert a decisive influence on the flow architecture, effectively modulating the transition between fluid penetration and redirection. At low *Da* values ($10^{-6} \leq Da \leq 10^{-4}$), the porous matrix behaves almost like a solid obstacle, forcing the flow around it. At high *Da* values ($10^{-3} \leq Da \leq 10^{-2}$), the porous layer becomes highly permeable, allowing significant fluid penetration and reducing its impact on flow organization.
- **Effect of Reynolds number (*Re*):** Increasing *Re* enhances ventilation effectiveness by accelerating the incoming airflow, thereby improving pollutant removal and heat extraction from the cavity.
- **Effect of Rayleigh number (*Ra*):** Higher *Ra* promotes buoyancy-driven transport, intensifying contaminant removal and contributing to improved depollution efficiency.
- **Effect of chemical reaction:** The reaction rate significantly influences species concentration fields, depollution efficiency, and the indoor air quality index. However, it does not affect hydrodynamic behavior, temperature fields, or thermal efficiency. Importantly, chemical reactions reduce air renewal time, contributing to potential energy savings in ventilation systems.

This work's primary contribution lies in its novel integration of sustainable indoor air quality (IAQ) management with high-fidelity numerical simulation. The current study utilizes a Lattice Boltzmann framework based on Multiple Relaxation Times (MRT-LBM) to simulate the integrated transport of heat and mass across a ventilated space containing a chemically active porous divider. Such a computational technique demonstrates superior performance in managing the intricate interfacial constraints and the interdependent physical phenomena characteristic of this configuration.

The robustness of this research is enhanced through an extensive parametric investigation, which rigorously evaluates the impact of critical dimensionless parameters. Specifically, the study assesses how the system's behavior is dictated by the Darcy (*Da*) number, the inertial effects represented by the Reynolds (*Re*) number, and the buoyancy-driven flow characterized by the Richardson (*Ri*) number, while also accounting for the kinetics of the chemical reaction rate (A_k). This extensive dataset moves beyond qualitative description to provide quantitative, actionable insights for engineers. Specifically, the results establish clear correlations between these parameters and system performance, offering a practical framework for optimizing ventilation strategies and reactive material selection to enhance depollution and thermal efficiency.

The research bridges a critical gap between mesoscopic computational fluid dynamics and applied building science. It demonstrates a viable pathway for designing ventilation systems that are not only energy-efficient, but also actively improve indoor air quality, thereby making a direct contribution to the creation of healthier and more sustainable built environments.

Outlook and Future Work: The findings of this research highlight the transformative potential of combining reactive porous dividers with optimized ventilation schemes. This integration emerges as a robust strategy for harmonizing thermal regulation with high-standard indoor air quality, offering a dual-benefit approach for modern building environments. Such a methodology resonates with the fundamental principles of sustainable architecture.

To transition these findings into practical applications, future research should focus on:

- Advance model: Progress from 2D to 3D simulations and from steady state to transient flow analysis.
- Expand chemical scope: Incorporate multi-species transport to understand performance with mixed pollutants.
- Deliver practical tools: Generate optimized design guidelines through comprehensive parametric analysis of key use cases.

9. ACKNOWLEDGEMENT

The paper is the result of the research accomplished in the frame of the PhD position of the first and second authors.

10. LIST OF ABBREVIATIONS

LBM-MRT: Lattice Boltzmann Method with Multiple Relaxation Time
IAQ: Indoor Air Quality Index
CFD: Computational Fluid Dynamics

C	Speed of sound	m/s
Da	Darcy's number	-
e	thickness of the separation	-
F	External forces	N
f	Distribution function	-
f^eq	Distribution function at equilibrium	-
g	Thermal distribution function	-
$\vec{g}$	Gravity acceleration vector	m/s
H	Cavity height	m
H_p	Height of the porous separation	-
HR	Relative humidity of the air	-
j	Components of angular momentum	(kg*m²)/s
k_{eff}	Porous medium conductivity	W/(m*K)
k_f	Fluid conductivity	W/(m*K)
K	Intrinsic permeability	m²
L	Cavity length	m
M	Transformation matrix	-
m	Gas Molecular weight	g/(mol*m)
m	Moments	-
m^{eq}	Moments of balance	-
Nu	Nusselt number	-
Pr	Prandtl number	-
Ra	Rayleigh number	-
Re	Reynolds number	-
Ri	Richardson number	-
T_h	Temperature hot	K
A_K	Dimensionless chem. reaction rate	-
t	Non-dimensional time	-
u	Non-dimensional longitudinal velocity	-
v	Vertical speed	m/s
V	Non-dimensional vertical velocity	-
x	Axial coordinates	m
X	Dimensionless axial coordinate	-
y	Vertical coordinate	m
Y	Non-dimensional vertical coordinate	-
A	Thermal diffusivity	m^2/s
B	Thermal expansion coefficient	K^{-1}
ε	Porosity	-
τ	Relaxation factor	-
ρ	Mass density	kg/m^3
μ	Dynamic viscosity of the fluid	Pa*s
μ_{eff}	Effective dynamic viscosity	Pa*s
Δt	Time step (increment)	s
$\Omega(f_i)$	The discrete collision operator	-
ϑ	Kinematic viscosity	m^2/s
ω	Collision frequency	-
w_i	Lattice constants	-
θ	Non-dimensional temperature	-

11. REFERENCES

[1] Y. Sun, J. Hou, R. Cheng, Y. Sheng, X. Zhang, J. Sundell, *Indoor air quality, ventilation and their associations with sick building syndrome in Chinese homes*, Energy Build, vol. 197, pp. 112–119, Aug. 2019, doi: 10.1016/j.enbuild.2019.05.046.

[2] H.-H. Liang, C.-P. Chen, R.-L. Hwang, W.-M. Shih, S.-C. Lo, H.-Y. Liao, *Satisfaction of occupants toward indoor environment quality of certified green office buildings in Taiwan*, Build Environ, vol. 72, pp. 232–242, Feb. 2014, doi: 10.1016/j.buildenv.2013.11.007.

[3] S. Sadrizadeh et al., *Indoor air quality and health in schools: A critical review for developing the roadmap for the future school environment*, Journal of Building Engineering,

vol. 57, p. 104908, Oct. 2022, doi: 10.1016/j.jobe.2022.104908.

[4] D.-M. Mustață, D. Bisorca, I. Ionel, A. Adjal, R.-M. Balogh, *Real-Time Insights into Indoor Air Quality in University Environments: PM and CO2 Monitoring*, Atmosphere (Basel), vol. 16, no. 8, p. 972, Aug. 2025, doi: 10.3390/atmos16080972.

[5] M. Pulimeno, P. Piscitelli, S. Colazzo, A. Colao, A. Miani, *Indoor air quality at school and students' performance: Recommendations of the UNESCO Chair on Health Education and Sustainable Development & the Italian Society of Environmental Medicine (SIMA)*, Health Promot Perspect, vol. 10, no. 3, pp. 169–174, Jul. 2020, doi: 10.34172/hpp.2020.29.

[6] A.-M. Sadick, Z.E. Kpamma, S. Agyefi-Mensah, *Impact of indoor environmental quality on job satisfaction and self-reported productivity of university employees in a tropical African climate*, Build Environ, vol. 181, p. 107102, Aug. 2020, doi: 10.1016/j.buildenv.2020.107102.

[7] Y. Kim, S. Hong, E. Yang, *Perceived productivity in open-plan design library: Exploring students' behaviors and perceptions*, J Learn Spaces, vol. 10, no. 3, pp. 28–42, 2021.

[8] C. Sun, X. Huang, J. Zhang, R. Lu, C. Su, C. Huang, *The new model for evaluating indoor air quality based on childhood allergic and respiratory diseases in Shanghai*, Build Environ, vol. 207, p. 108410, Jan. 2022, doi: 10.1016/j.buildenv.2021.108410.

[9] G. Gan, *Simulation of buoyancy-driven natural ventilation of buildings—Impact of computational domain*, Energy Build, vol. 42, no. 8, pp. 1290–1300, Aug. 2010, doi: 10.1016/j.enbuild.2010.02.022.

[10] S.A. Al-Sanea, M.F. Zedan, M.B. Al-Harbi, *Heat transfer characteristics in air-conditioned rooms using mixing air-distribution system under mixed convection conditions,* International Journal of Thermal Sciences, vol. 59, pp. 247–259, Sep. 2012, doi: 10.1016/j.ijthermalsci.2012.04.023.

[11] L. Nasseri, O. Rahli, D.E. Ameziani, R. Bennacer, *Study of mixed convection in closed enclosure with a ceiling fan*, The European Physical Journal Applied Physics, vol. 86, no. 2, p. 20902, May 2019, doi: 10.1051/epjap/2019190045.

[12] H.F. Oztop, K. Al-Salem, Y. Varol, I. Pop, *Natural convection heat transfer in a partially opened cavity filled with porous media*, Int J Heat Mass Transf, vol. 54, no. 11–12, pp. 2253–2261, May 2011, doi: 10.1016/j.ijheatmasstransfer.2011.02.040

[13] N. Himrane, D.E. Ameziani, K. Bouhadef, R. Bennacer, *Storage Silos Self Ventilation: Interlinked Heat and Mass Transfer Phenomenon*, Numeri Heat Transf A Appl, vol. 66, no. 4, pp. 379–401, Aug. 2014, doi: 10.1080/10407782.2014.884891.

[14] L. Nasseri, O. Rahli, D.E. Ameziani, R. Bennacer, *Study of mixed convection in closed enclosure with a ceiling fan*, The European Physical Journal Applied Physics, vol. 86, no. 2, p. 20902, May 2019, doi: 10.1051/epjap/2019190045.

[15] Q. Liu, Y.-L. He, Q. Li, W.-Q. Tao*, A multiple-relaxation-time lattice Boltzmann model for convection heat transfer in porous media*, Int J Heat Mass Transf, vol. 73, pp. 761–775, Jun. 2014, doi: 10.1016/j.ijheatmasstransfer.2014.02.047.

[16] A. Arab, N. Himrane, D E. Ameziani, Z. Hireche, Y. Halouane, M. Magherbi, *LBM-MRT study of a reactive porous separation on thermal and depollution efficiency in a ventilated room*, International Communications in Heat and Mass Transfer, vol. 155, p. 107585, Jun. 2024, doi: 10.1016/j.icheatmasstransfer.2024.107585.

[17] A. Arab, N. Himrane, Z. Hireche, Y. Halouane, R. Bennacer, D.E. Ameziani, *Analysis of a reactive porous separation effects on depollution and indoor air quality: Application of LBM-MRT to heat and mass transfers,* International Journal of Thermal Sciences, vol. 197, p. 108754, Mar. 2024, doi: 10.1016/j.ijthermalsci.2023.108754.

[18] D.D. Gray, A. Giorgini, *The validity of the boussinesq approximation for liquids and gases*, Int J Heat Mass Transf, vol. 19, no. 5, pp. 545–551, May 1976, doi: 10.1016/0017-9310(76)90168-X.

[19] A. Bejan, *Convection Heat Transfer*. Wiley, 2013. doi: 10.1002/9781118671627.

[20] F.M. White, S.A. Klein, *Fluid mechanics*. McGraw Hill, 2011.

[21] A.S. Lavine, D.P. DeWitt, *Fundamentals of Heat and Mass Transfer*. Wiley, 2020.

[22] C. Cercignani, A.S. Berman, *Theory and Application of the Boltzmann Equation*, J Appl Mech, vol. 43, no. 3, pp. 521–521, Sep. 1976, doi: 10.1115/1.3423913.

[23] U. Frisch, B. Hasslacher, Y. Pomeau, *Lattice-gas automata for the Navier-Stokes equation*, Phys. Rev. Lett., vol. 56, no. 14, pp. 1505–1508, Apr. 1986, doi: 10.1103/PhysRevLett.56.1505.

[24] S. Chapman, T G. Cowling, D. Park, *The Mathematical Theory of Non-Uniform Gases*, Am J Phys, vol. 30, no. 5, pp. 389–389, May 1962, doi: 10.1119/1.1942035.

[25] P.L. Bhatnagar, E.P. Gross, M. Krook, *A Model for Collision Processes in Gases. I. Small Amplitude Processes in Charged and Neutral One-Component Systems*, Physical Review, vol. 94, no. 3, pp. 511–525, May 1954, doi: 10.1103/PhysRev.94.511.

[26] N. Shah, P. Dhar, S.K. Chinige, M. Geier, A. Pattamatta, *Cascaded collision lattice Boltzmann model (CLBM) for simulating fluid and heat transport in porous media*, Numerical Heat Transfer, Part B: Fundamentals, vol. 72, no. 3, pp. 211–232, Sep. 2017, doi: 10.1080/10407790.2017. 1377530.

Managementul durabil al calității aerului interior: un studiu numeric al transferului de căldură și masă în cavități ventilate utilizând metoda LB-MRT

Studiul investighează transportul căldurii și masă într-o incintă dreptunghiulară ventilată, utilizând modelare numerică. Obiectivul principal este optimizarea condițiilor aerului interior și a eficienței extracției contaminanților. Un aspect distinctiv al studiului constă în integrarea principiilor de management al sustenabilității în evaluarea numerică. Modelul fizic include o barieră poroasă reactivă centrală, cu permeabilitate ajustabilă, pentru a simula procesele de filtrare. Prin investigarea diferitelor strategii de ventilație pentru spații rezidențiale, studiul evaluează confortul termic și purificarea aerului. Analiza se bazează pe modele de curgere, distribuțiile termice și gradienții de concentrație, alături de indicatori de performanță precum gradul de depoluare și indicatorii calității aerului.

Ahmed ADJAL, PhD student, Universitatea Politehnica Timișoara, Faculty for Mechanical Engineering, ahmed.adjal@student.upt.ro, Timisoara, Romania

Venera Stanca NICOLICI, PhD student, Universitatea Politehnica Timișoara, Faculty for Mechanical Engineering, venera-stanca.morar@student.upt.ro, Timisoara, Romania

Ioana IONEL, PhD., Professor, Universitatea Politehnica Timișoara, Faculty for Mechanical Engineering, ioana.ionel@upt.ro, Timisoara, Romania

Daniel BISORCA, PhD., Lecturer, Universitatea Politehnica Timișoara, Faculty for Civil Engineering, daniel.bisorca@upt.ro, Timisoara, Romania